

Indentation Based Determination of Mechanical Properties of Materials

Michael V Swain

CSIRO Division of Applied Physics,
Lindfield NSW 2070 Australia

Indentation methods have been used for over a century now to determine the hardness of materials. However, despite this widespread use only limited information has been gleaned from the material indented. This has arisen because the usual methods of analysis only evaluate the residual impression dimensions rather than the entire load-displacement trace of the indentation event. The recent emphasis of ultra-micro or nano-indentation systems has limited the ability to make such measurements because of the size of the residual impressions. Instead analysis of the millinewton-nanometre data is required to determine hardness and modulus. Until recently nearly all indentation studies were made with triangular pyramid diamond Berkovich indenters. However, it has been shown recently that more fundamental behaviour of materials can be determined using spherical tipped indenters of micron radii. With these indenters the elastic/plastic or brittle transition may be followed to determine the hardness (or mean pressure), elastic modulus and stress-strain behaviour. Examples of the application of this approach to ceramics, metals, polymers and thin films will be given along with the identification of fundamental phase transformations in semi-conducting silicon during indentation. Also examples of indentation induced delamination of thin films on various substrates are given.

1. INTRODUCTION

Indentation methods have been widely used for investigation of mechanical properties of materials for a long time. Very often, hardness is measured, which provides information about the resistance of a material against penetration by another body. The measurement consists of pressing a hard indenter by a defined force into the test specimen and measuring the remnant imprint in the material after unloading. Usually, hardness is given as

$$H = P/A \quad (1)$$

where P is the load, and A - area of the permanent imprint.

The advantage of this kind of test is that it is a simple procedure with minimal specimen requirements (no special shape, one specimen can be used for several indentations, the specimen is not always destroyed, only locally damaged). Moreover, the characteristic stressing during indentation is similar to many real situations (contact with other

bodies or particles, abrasion, wear, machining, etc.).

Originally, indentation methods were used to estimate the hardness of ductile, usually metallic materials. With technological development the field of their applicability has greatly increased. The need for a simple method of investigation of the mechanical properties of brittle materials led to the development of micro-hardness testers, with load ranges from 0.1 N to several N, and characteristic dimensions of the imprint in μm . With these devices, it could be recognised that even such a brittle material as glass may be plastically deformed in microscopically small volumes.

More recently, the need to study mechanical properties of surface engineered components, has necessitated the development of so-called ultra micro-hardness testers, which use loads of only mN and are able to measure impressions only some nanometres deep. Especially with thin films deposited on the surface in order to achieve special properties; mechanical, electrical or optical. This was also made possible due to improvements in precision measurement technology, and due to the use of

computers for measurement control and data processing. In order to obtain as much information as possible, indenter load and displacement are measured during loading and unloading (Fig. 1a). Some of these mechanical property micro-probe systems, like the UMIS-2000 [1] make it possible for stepwise loading with partial unloading between individual steps (Fig. 1b). This kind of measurement, producing P- δ (load-penetration) curves, enables one to determine not only hardness, but also the elastic modulus, stress-strain response (and how they depend on dimensions of the imprint). In this manner it is possible to reveal various processes and changes within the material, like pressure-induced phase transformations, initiation of cracks, etc. (Fig. 2).

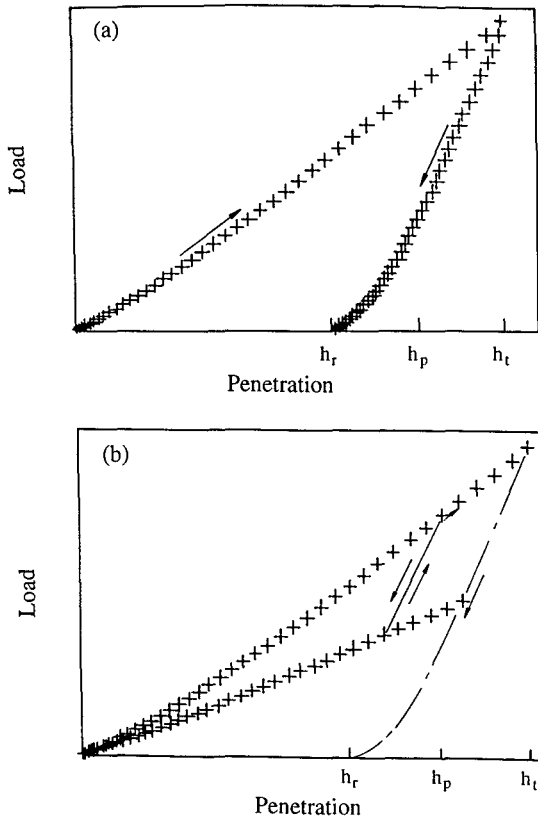


Fig. 1 (a) Load cycle plot typical of an elastic-plastic material such as steel. (b) Multiple partial unloading plot.

The shortcoming of indentation methods occurs because of the strongly inhomogeneous stress field in the area of investigation. As a result, various methods for evaluation of results and determination

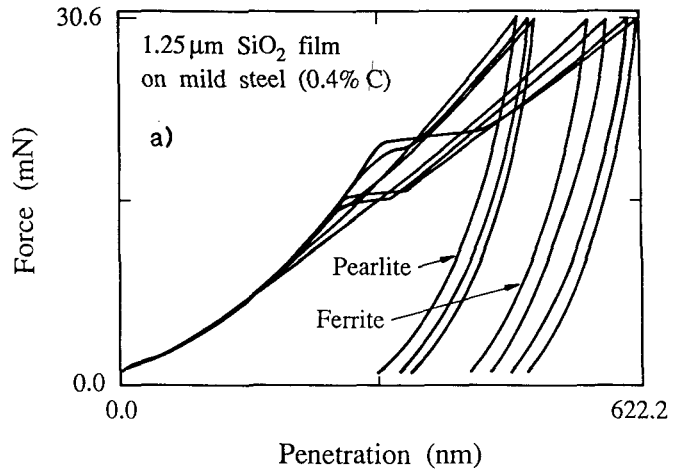


Fig. 2 Load-displacement data for a silica film on a steel substrate. Berkovich indenter; the horizontal part of the curves corresponds to film fracture.

of material characteristics have been developed and used-from simple, often semi-empirical, to more sophisticated and complicated. The choice of a particular method depends on the material and property to be determined, and on the measuring techniques and system used. It also depends among other things, on the form of the indenter. For example, a pointed indenter, like a Vickers or Berkovich creates a permanent deformation in the specimen almost at the onset of loading, with complicated relationships between stresses and strain. On the other hand, a spherical-tipped indenter (with the tip radius of several μm) produces a purely elastic deformation initially and the force-displacement relationships for this case are relatively simple and well known. For example, the depth of penetration is given by the formula

$$\delta = (9/16)^{1/3} (1/R)^{1/3} (P/E^*)^{2/3} \tag{2}$$

where R = radius of the indenter, and E^* the effective elastic modulus of the contacting pair, defined by

$$1/E^* = (1-\nu_i^2)/E_i + (1-\nu_s^2)/E_s \tag{3}$$

where E_i , E_t and ν_i, ν_t are Young's modulus and Poisson's ratio for the indenter and tested materials, respectively. After fitting the relationship (2) to the values $P(\delta)$ obtained, the effective modulus E^* can be determined, from which again, the modulus E_t (or $E_t/(1-\nu_t^2)$) of the tested material can be found (supposing E_i, ν_i of the indenter are known). Of course, the relationship (2) is valid only up to the moment when the maximum contact stress reaches the yield point σ_Y . With higher loads, the situation is more complex, and the calculations must be modified [2].

A method for determination of the elastic modulus uses the fact that in the case of deep impressions (i.e. with relatively large amount of plastic deformation), the contact area remains unchanged during the initial stages of unloading, so that the relationship $P(\delta)$ is linear (Fig. 1a),

$$\frac{dP}{d\delta} = \beta\sqrt{AE^*} \tag{4}$$

where A is the surface area of the imprint, and β is a constant depending on the kind of indenter used, Vickers or Berkovich [3]. For a spherical indenter, Field and Swain [2] have found the relationship

$$E^* = kP/(a\delta) \tag{5}$$

where a is the radius of contact and δ is the depth of the imprint as may be determined by partial unloading, and k ($\approx 3/4$) is a constant.

A very important problem is the determination of properties of thin films. The substrate with its properties (E, σ_Y, H, \dots) influences the measured film behaviour, more particularly with thinner films. This is also reflected in indentation measurements: the measured values depend, among other things, on the relative depth of the imprint.

Generally, the values of elastic modulus, hardness, etc. measured at very small depths of impression (compared with the film thickness), the influence of substrate properties is not so critical (Fig. 3). Moreover, the character of the strain field, which is decisive for the total response of a structure (film-substrate), may be very different in the case of a ductile film on a hard substrate, or a hard, brittle film

on a soft substrate (Fig. 4). This complicates the evaluation of measurement. The general response, $P(\delta)$, of such a structure under local loading can be found quite easily, but the determination of particular properties of the film alone may be difficult. There are several approaches to the problem. For example, Bhattacharya and Nix [4], starting from finite element elastic-plastic modelling of various film-substrate combinations, proposed the following expressions for the apparent (measured) hardness:

(a) soft film on a harder substrate

$$\frac{H}{H_s} = 1 + \left(\frac{H_f}{H_s} - 1 \right) \exp \left[- \frac{\sigma_{Yf}/\sigma_{Ys}}{E_f/E_s} \left(\frac{\delta}{h} \right)^2 \right] \tag{6}$$

(b) hard film on a softer substrate

$$\frac{H}{H_s} = 1 + \left(\frac{H_f}{H_s} - 1 \right) \exp \left[- \frac{H_f/H_s}{(\sigma_{Yf}/\sigma_{Ys})\sqrt{(E_f/E_s)}} \left(\frac{\delta}{h} \right)^2 \right]$$

If we perform several measurements of hardness to various depths of indentation, we can fit the measured values H by the function (6) or (7), and, having known properties of the substrate, determine the hardness, elastic modulus, etc., corresponding to the film above. In the above-mentioned study [4], starting from a-priori given values of $E_f, E_s, \sigma_{Yf}, \sigma_{Ys}, \dots$, the agreement between the observations generated by finite element modelling and those obtained using Eqs (6), (7) was quite good. With real measurement, however, especially when Eqs (6), (7) are used for prediction of properties outside the range of values used for their determination, the results may be less reliable [5]. The main reason is perhaps, that the functions of E_f/E_s and σ_{Yf}/σ_{Ys} in Eqs (6), (7) do not represent physical laws but are more a mathematical expression of observed trends.

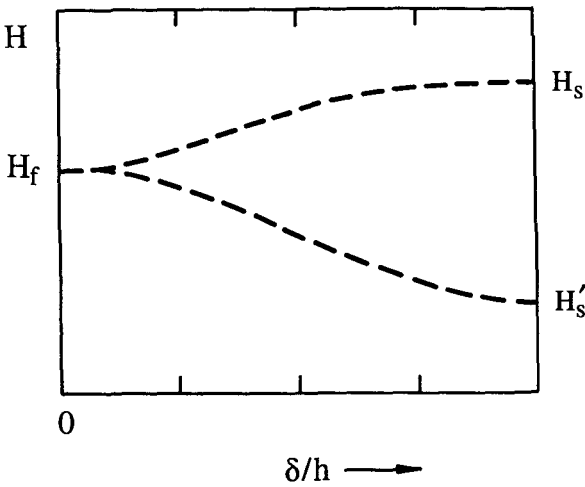


Fig. 3 Apparent hardness (H) of a film-substrate as a function of relative depth of indentation (δ/h) with h the film thickness; subscripts f , s denote film and substrate, respectively.

As for hardness, there are many papers suggesting, in principle, that the apparent hardness of a film-substrate structure is determined by a weighted average of the volume of a plastically deformed material in the film (V_f) and in the substrate (V_s). The simplest formula,

$$H = \frac{H_f V_f + H_s V_s}{V_f + V_s} \tag{8}$$

originally proposed by Sargent [6], was later modified in several ways to include the influence of further material characteristics and the extent of deformation developed; see, e.g. [5]. It has also been argued that not only the indentation depth but also the radius of contact area (together with the film thickness) play an important role.

The formulae like (8) can be used to determine (with more or less accuracy) the true hardness of the film. However, these formulas say nothing about other film properties like e.g. elastic modulus. As we have seen in Eqs (6), (7), an attempt to formulate a universal expression involving elastic and plastic properties of the structure, need not always lead to the best results. At this time, it seems more suitable to use various parts of the $P(\delta)$ diagram and various methods for determination of plastic or elastic

characteristics of the film. As for elastic modulus, several approaches have again been proposed [7-9]. The more promising seem to be the methods based on the theory of contact of a rigid cylindrical punch indenting elastic half space with one or more layers on its surface. Regardless of the assumption of elastic behaviour, the solution may also be used with some caution for indentation tests with plastic deformation, because during the initial stage of unloading (and reloading) the contact area remains unchanged and the relationship between load and displacement is linear. The solution of Gao *et al.*[8] corresponds more closely to experiments in the sense that it uses the weight function approach expressing the contributions of individual layer's stiffnesses (and energy) to the total stiffness (and energy). Moreover, the final expressions are relatively simple and easy to use.

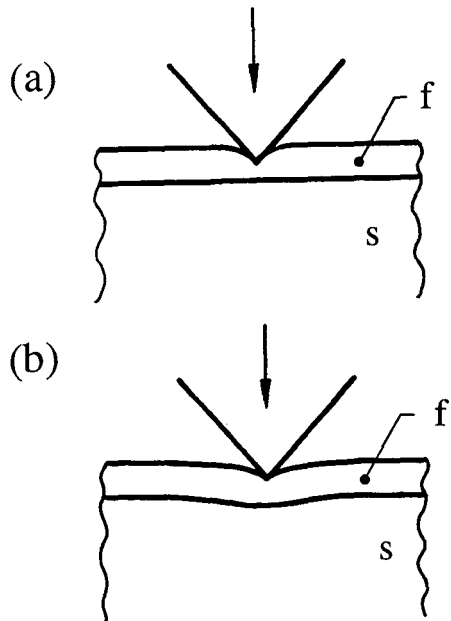


Fig. 4. Typical behaviour of a soft film on a hard substrate (a), and a hard film on a soft substrate (b).

When speaking about these various approaches, a question can be raised; to what degree are measurements necessary, and at what degree can they be replaced by mathematical modelling? In fact, the finite element method, for example, represents a

very powerful tool to study the behaviour of various structures and materials. Unfortunately, every such model requires a constitutive relationship for the mechanical properties of the materials being measured. In materials research, however, and in thin films technology especially, there is a great diversity of properties and their combinations, and their FEM modelling could last too long in some cases, especially if we include the nonlinear material behaviour and changes in contact area with the load. Moreover, in the case of brittle materials (e.g. brittle film on a tough substrate, or a ductile film on a brittle substrate), destructive processes in the material occur at a certain load (cracking of the film or substrate, delamination), and no continuum models can exactly forecast them. On the contrary, if the behaviour of a certain material is principally known, it is possible to investigate its properties more thoroughly using mathematical modelling. The experimental investigation and observation, however, is of primary importance. This is also why simple models (that reflect the physical nature of the problem) are often preferred for determination of material properties (E , σ_y ,...) from the measured $P(\delta)$ data. Such models also allow quick processing of the data generated on a PC, which is usually a part of the measuring facility. Examples of such measurements and evaluation will be given in the following section.

In this paper examples of the applicability of indentation methods to measure the mechanical properties of metallic, polymeric and brittle materials. Emphasis will be placed on the novel use of small spherical tipped indenters to measure these properties. This will be followed by observations on a variety of thin films.

2. OBSERVATIONS AND DISCUSSION

Measurements of the force-displacement behaviour of the various materials mentioned below were made with a commercially available UMIS-2000 ultra micro-indentation systems which has been described elsewhere [1].

2.1 Metals

a) Steels

Measurements of the force-displacement response

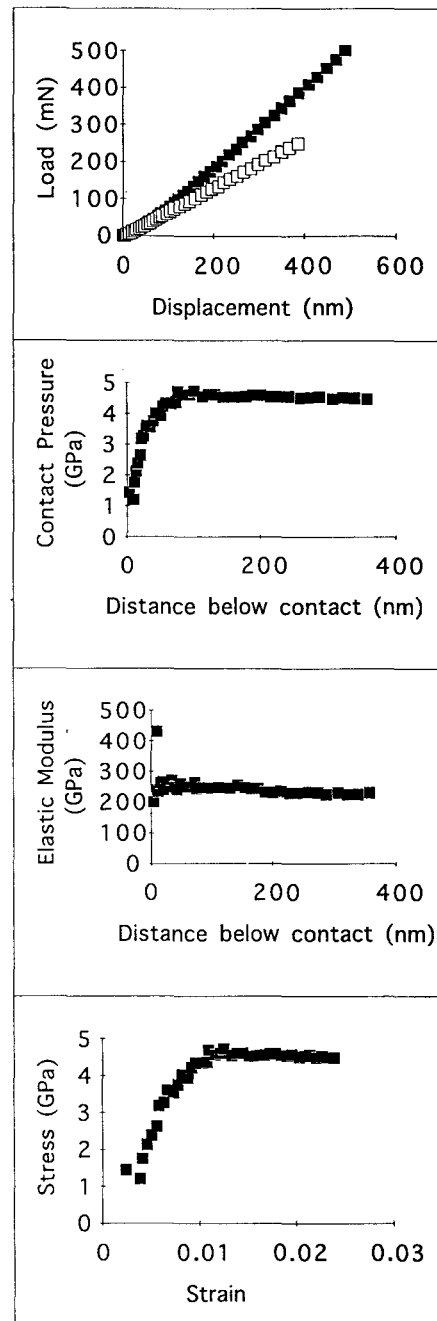


Figure 5 a) Force-displacement data generated with a 50 μm radius indenter on a steel hardness block of nominal hardness 500 kg/mm^2 . b) Contact press and c) elastic modulus variation with depth of penetration, and d) stress-strain response.

upon using the load partial unload procedure on a steel hardness block of nominal value 500 kg/mm^2 .

The data shown in Figure 5a was taken using a 50 μm radius indenter. The initial response is elastic as may be appreciated from the overlap upon unloading. Analysis of the data for hardness versus depth and elastic modulus is shown in Figures 5b and c. The material exhibits almost constant hardness $\sim 5\text{GPa}$ as anticipated without any evidence of work hardening. The latter behaviour is also apparent in Figure 5d which plots the stress strain response.

b) Glassy Metals

These materials have attracted considerable interest because of their wide applicability from transformer windings to high strength micro crystalline metals and low temperature reactive brazing materials. However very little information about the elastic-plastic response of them is available as the presence of defects at the edge often means they fail in a brittle manner before yield occurs when loaded in tension. The indentation response of a 20 μm thick film loaded with a 2 μm radius indenter are shown in Figure 6. The analysis of this data is shown in Figures 6b - d.

c) $\text{Ti}_3\text{Al-Nb}$ Alloy

These materials have attracted considerable interest over the last decade because of their excellent potential for high temperature applications. Of all the Ti_3Al alloys the addition of Nb has been found to improve the room temperature ductility. As shown by Kim et al [15] this alloy may be heat treated to develop a wide range of microstructures. In this paper we shall only consider a suddenly quench SQ material that has been held above the $\alpha_2 - \beta$ phase boundary at 1100°C . The influence of various heat treatments on the microstructure developments, ductility and properties of the various phases is discussed elsewhere [12].

Observations of the force-displacement data obtained with a 5 μm radius indenter and its analysis to determine mean-contact pressure (or hardness) and elastic modulus with depth are shown in Figures 7a - c. The interpretation of the mean contact pressure versus depth in terms of a stress-strain response is shown in Figure 7d. This last figure shows a rapidly work hardening curve - very different from those generated with the low carbon steel: in Figures 5

More critical appraisal of the data in Figure 7a should attempt to accommodate for the severe work

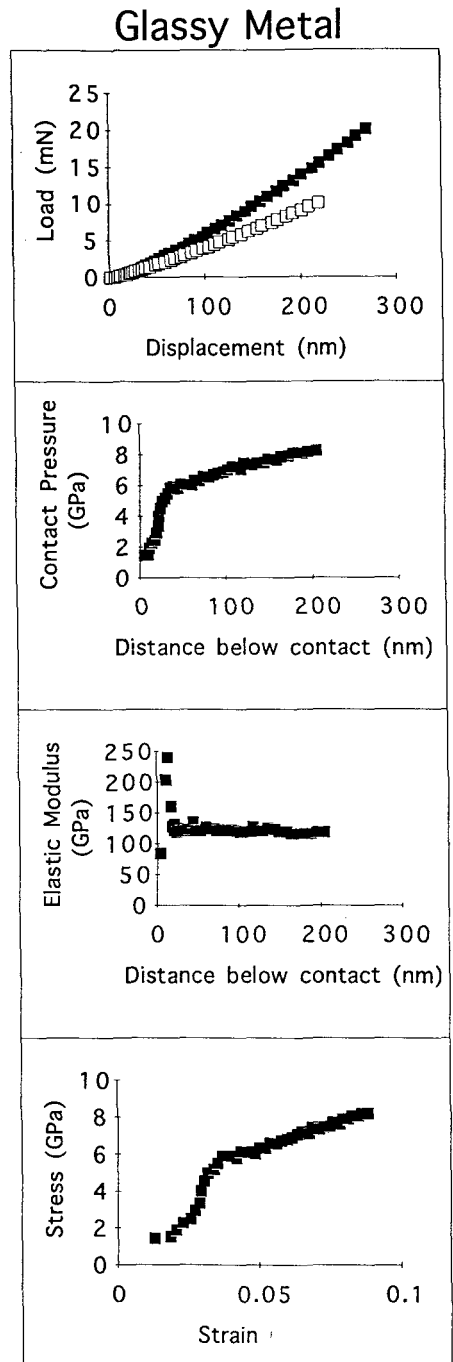


Figure 6 a) Force-displacement data generated on a glassy metal with a 2 μm radius indenter. b) Contact pressure and c) elastic modulus variation with depth of penetration, and d) stress-strain response.

hardening which will develop pile up about the impression and lead to errors in the determination of the contact diameter. This consideration is currently being addressed by Field in Swain [18] using an approach pioneered by Norbury and Samuels [19].

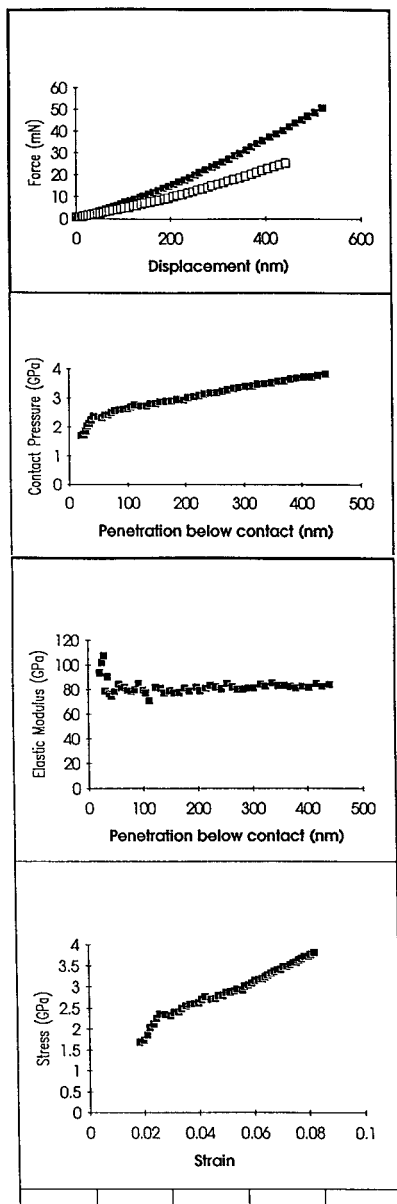


Figure 7 a) Force-displacement data generated with a 5 μm radius indenter on a $\text{Ti}_3\text{Al-Nb}$ alloy suddenly quenched from 1100°C. b) Contact pressure and c) elastic modulus variation with depth of penetration, and d) stress-strain response.

d) Polymers

The indentation response of polymers is somewhat more complex than that of elastic-plastic materials in that visco-elastic behaviour often occurs. In this paper such issues will not be addressed and an example of the response of a dry PMMA based hydrogel is given. These materials find wide application as contact lenses.

Observations of the force-displacement response of these hydrogel indented with a μm radius indenter are shown in Figure 8a. The variation of the mean contact pressure, modulus with depth are shown in Figures 8b and c. The stress-strain response is shown in Figure 8d. The hydrogel material exhibits almost classic elastic-plastic response and has an E modulus close to GPa.

e) Brittle Material

As a classic example of a brittle material we shall consider the indentation response of single crystalline silicon. This has been considered in more detail by Weppelmann et al [13]. The indentation response of silicon with pointed indenters is somewhat controversial as the material exhibits hysteretic response and cracking even at very low loads. However indentation with a spherical tipped indenter provides a more readily analysable response.

A continuous force-displacement indentation response with 10 μm radius tipped diamond indenter is shown in Figure 9a. The curve shows an initial elastic response up to ~ 75 nN and then plastic response. The continuous broken line is the anticipated elastic response from equation (2). Upon unloading the curve exhibits a "pop-out" event before continuing to smoothly unload. This behaviour may be simulated as shown in Figure 9b by considering the material behaves elastically up to a mean contact pressure of $\sim 11 - 11.5$ GPa where upon it behaves "plastically". On unloading the material behaves elastically until the mean pressure reduces to $\sim 8 - 9$ GPa when the "pop-out" event occurs. These two critical pressures 11 GPa and 8 GPa correspond to the hydrostatic phase transformation pressures of silicon from its normal semi-conducting structure (Silicon I) to a metallic structure (Silicon II) with a 22% volumetric collapse of the unit cell and upon unloading to an intermediate phase (Silicon III). The hardness of silicon may therefore be associated with a pressure induced phase transformation.

Hydrogel

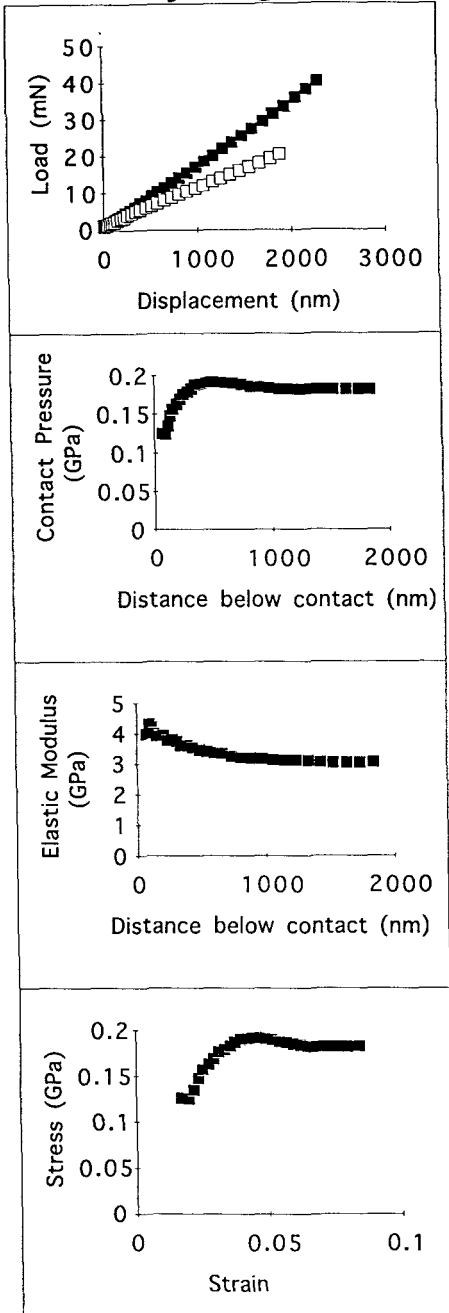


Figure 8 a) Force-displacement data obtained on a polymeric PMMA based hydrogel (dry) with a $1\ \mu\text{m}$ radius indenter b) Contact pressure and c) elastic modulus variation with depth of penetration, and d) stress-strain response.

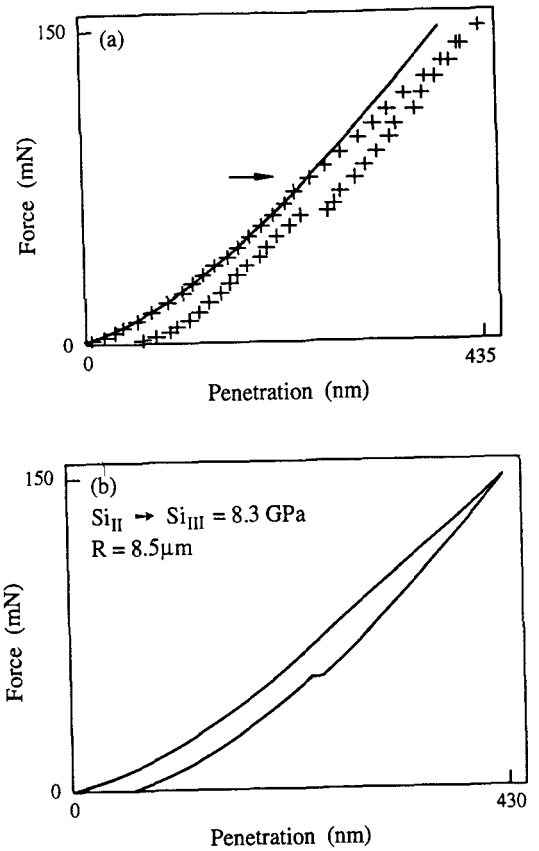


Figure 9.a) Continuous force-displacement data obtained during indentation of silicon with a $10\ \mu\text{m}$ nominal radius indenter. Crosses data broken line anticipated elastic response. b) Simulation of the force-displacement data assuming the onset of "plasticity" at 11.5 GPa and reverse phase transformation at $\sim 8\ \text{GPa}$.

f) Films Platinum on Silicon

Observations have been made of the mechanical properties of $1\ \mu\text{m}$ thick platinum films deposited on silicon using an unbalanced magnetron sputtering technique. Indentations were made with a $5\ \mu\text{m}$ radius indenter. The calculated values of the mean contact pressure and modulus with depth are shown in Figure 10 a and b. The initial elastic response and then strain-softening before work hardening occurred was found to be a function of the deposition

Platinum on Silicon

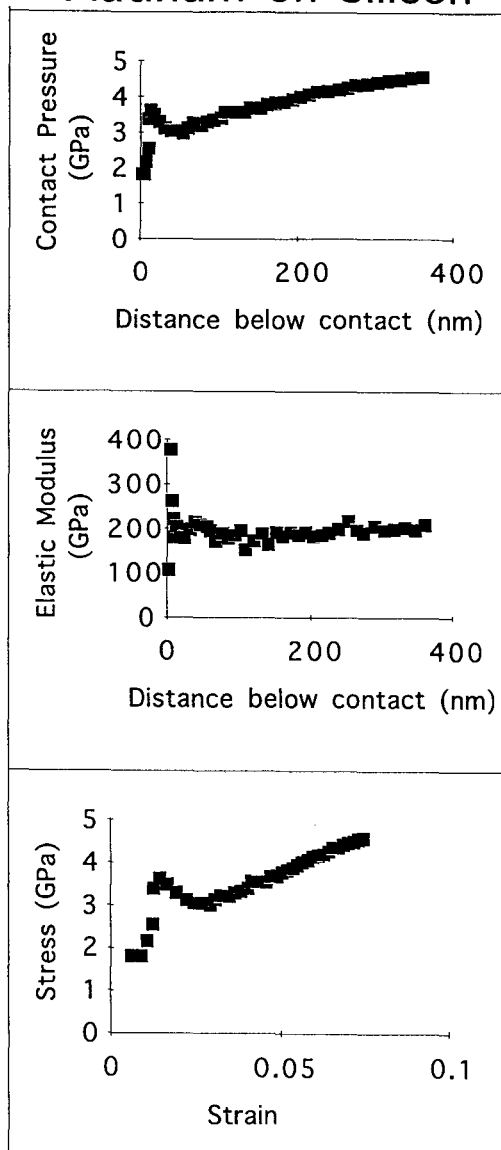


Figure 10 Variation of the mean contact pressure of a platinum film on silicon a), and elastic modulus b) with depth of penetration.

conditions and will be discussed in detail elsewhere by Tokura et al [17]. Similar initial elastic response and strain softening was observed by Bell et al [16] of Al/Cu films on silicon. In the latter paper it was suggested this behaviour was due to an oxide layer.

Polyimide Films on Glass

Polyimide films are now widely used in situations where extreme thermal and mechanical conditions for a polymer prevail. They are also finding every increasing applications in the micro-electronics industry particularly where multi-layer coatings are required. Rather than show curves similar to those seen for the polymer hydrogels in Figure 8 above, we shall just quote the typical modulus and hardness values for this material, namely 8 GPa and 0.7 GPa respectively for a 2 micron thick film. However it was found that if a larger radius indenter was used then delamination of the film occurred. A typical example of the response of a 2 μm film indented with a 20 μm radius indenter are shown in Figure 11. This figure shows the superposition of a number of continuous force displacement curves to heavier loads, the step discontinuity marks the onset of film delamination. These observations may be interpreted to determine the maximum interfacial shear stress to initiate film fracture following Matthewson [14]. Also if one can measure the size of the delaminated zone the interfacial fracture toughness may be estimated.

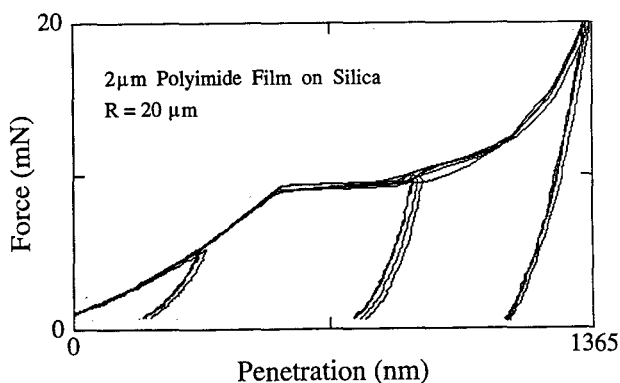


Figure.11. Superposition of multiple force-displacement data generated at different loads with a 20 μm radius indenter loaded into a 2 μm thick polyimide film on a silica glass substrate.

2.2 Tantalum Oxide on Glass and Silicon

Tantalum oxide is often used as a protective film on optical elements yet relatively little is known of its mechanical properties and the influence of deposition parameters. Recently Martin *et al.* [10] investigated the influence of a number of parameters

associated with ion assisted deposition (IAD) of 1 μm films of tantalum oxide films on glass and silicon. It was found that bias voltage had a significant effect on the parameters of density, refractive index and hardness. The UMIS enabled the determination of hardness or mean pressure and modulus with depth for films simultaneously deposited on glass and silicon substrates (E modulus of the substrates being 70 and 170 GPa, respectively). The variation of mean contact pressure with depth are shown in Fig. 12. The film on glass shows almost constant hardness whereas that on silicon appears to increase with depth of penetration as might be expected because of the relative hardness of the substrates (5 and 12 GPa for glass and silicon, respectively). These observations are currently being interpreted on the basis of the analysis by Gao *et al.* [8] to determine the E modulus of the tantalum oxide.

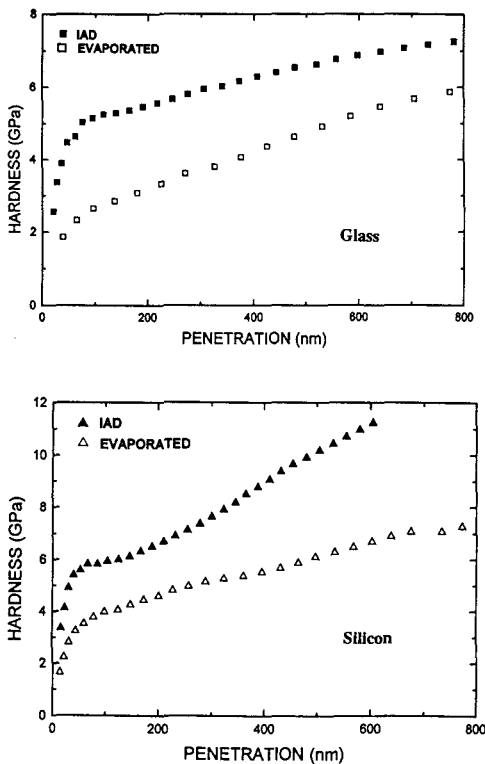


Figure 12. Comparison of the estimated mean contact pressure obtained with a 5 μm radius indenter versus depth of penetration for a 1 μm thick tantalum oxide film on glass and silicon substrates.

2.3 Titanium Nitride Films on Silicon

Examples of the behaviour of a 2.7 μm film of TiN indented with a 10 μm radius spherical indenter are shown in Fig. 13. These observations clearly show that at low loads the behaviour is entirely elastic, but upon exceeding a critical load film cracking occurs which continues at elevated loads. A similar behaviour may be observed with a pointed indenter. SEM observations of a cross-section of an impression indicate that no plastic deformation of the film occurred but only vertical faulting, all the inelastic deformation being accommodated in the silicon substrate. Interfacial delamination was also observed [11]. These observations suggest considerable care should be exercised before interpreting load-displacement data. The data in Fig. 13 before cracking do enable the E modulus of the film to be determined following the procedure outlined by Gao *et al.* [8].

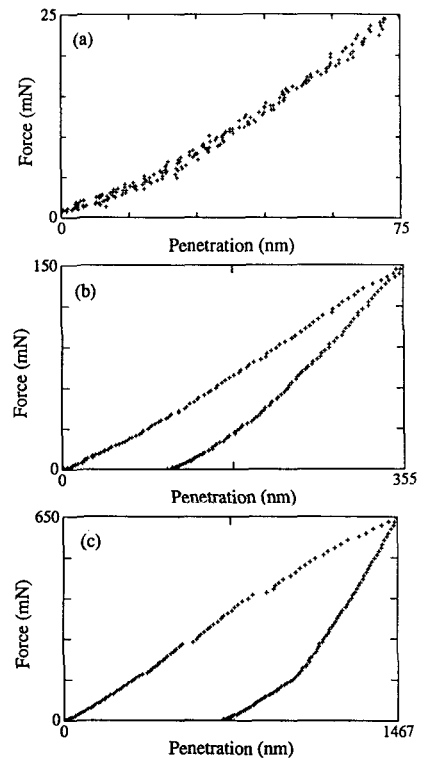


Figure 13. Force-displacement data generated on a 2.7 μm thick TiN film on silicon with a 5 μm radius indenter. Note the transition from elastic response to elastic-plastic-brittle behaviour with breaks the curve due to film fracture.

3. CONCLUSIONS

This paper has illustrated the usefulness of mechanical micro-probe systems to investigate the mechanical properties of a broad range of materials and thin films. This area is undergoing considerable development from both a theoretical and experimental perspective.

4. ACKNOWLEDGEMENTS

The author wishes to thank his many colleagues at CSIRO and E. Weppelmann and J. Mencik for their assistance in this research.

REFERENCES

1. Bell, T.J., Bendeli, A., Field, J.S., Swain, M.V., Thwaite, E.J., *Metrologia* **28**, 463 (1991/92).
2. Field, J.S., Swain, M.V., *J. Mater. Res.* **8**, 297 (1993).
3. Nix, W.D., *Metall. Trans.* **20A**, 2277 (1989).
4. Bhattacharya, A.K., Nix, W.D., *Int. J. Solids Structures*, **24**, 1287 (1988).
5. Fabes, B.D., Oliver, W.C., McKee, R.A., Walker, F.J., *J. Mater. Res.* **7**, 3056 (1992).
6. Sargent, P.M., in *Microindentation Techniques in Materials Science and Engineering* (edited by P.J. Blau and B.R. Lawn), ASTM STP 889, Philadelphia PA, 1986.
7. King, R.B., *Int. J. Solids Structures* **23**, 1657 (1987).
8. Gao, H., Chiu, Ch. H., Lee, J., *Int. J. Solids Structures* **29**, 2471 (1992).
9. Yu, H.Y., Sanday, S.C., Rath, B.B., *J. Mech. Phys. Solids*, **38**, 745 (1990).
10. Martin, P.J., Bendavid, A., Swain, M.V., Netterfield, R.P., Kinder, T.J., Sainty, W.G., Drage, N.D., *Mat. Res. Soc., Proc. San Francisco Meeting April 1993*.
11. Weppelmann, E.R., Hu, X-C., Swain, M.V., *Int. J. Adhesion Sci. and Tech.* in press.
12. Swain M.V. and Kim N. J., *SAMPE meeting December 1993*.
13. Weppelmann E.R., Field J.S., Swain M.V., and *J. Mater. Res.* **8**, 830 (1993).
14. Matthewson M.J., *Appl. Phys. Lett.* **49**, 1427 (1986).
15. Kim N.J., Kim J.Y., Lee D.Y., and Cho W.S., pp 467 *Light Weight Alloys etc.*
16. Bell T.J., Field J.S. and Swain M.V., *Thin Solid Films* **220**, 289 (1992).
17. Tokura H., Window B. and Swain M.V. in preparation.
18. Field J.S. and Swain M.V. in preparation.
19. Norbury A.L. and Samuels T., *Iron Steel Inst.* **117**, 673 (1928).